Self-trapping and multiplication of electronic excitations in Al_2O_3 and Al_2O_3:Sc crystals

M. Kirm and G. Zimmerer
II. Institute of Experimental Physics, University of Hamburg, Luruper Chaussee 149, D-22761 Hamburg, Germany

E. Feldbach, A. Lushchik, Ch. Lushchik, and F. Savikhin
Institute of Physics, University of Tartu, Riia 142, 51014 Tartu, Estonia
(Received 30 November 1998; revised manuscript received 10 March 1999)

The processes of intrinsic and extrinsic luminescence excitation by synchrotron radiation of 4–40 eV or electron pulses have been studied in α-Al_2O_3 single crystals at 8 K. The intrinsic *A* (7.6 eV) and *E* emissions (3.77 eV) can be effectively excited in the region of long-wavelength (8.85–9.1 eV) and short-wavelength (9.1–9.3 eV) components of exciton absorption doublet, respectively. Fast (~6 and ~20 ns) and slow (~150 ns) components of the *A* emission correspond to the creation of singlet and triplet p^5s excitons. The efficiency of the *A* emission in the region of band-to-band transitions is low. The intensity of *A* emission sharply increases (approximately quadratically) with a rise of the excitation density by nanosecond electron pulses. In Al_2O_3:Sc, the 5.6-eV luminescence is caused by the decay of near-impurity electronic excitations (~8.5 eV) as well as by the electron recombination with holes localized near Sc^{3+} centers. The efficiency of 7.6-, 5.6-, and 3.8-eV emission sharply increases at the energy of exciting photons of $h\nu > 25$ eV. One photon of 26–29 and 30–37 eV causes the ionization of the $2p^6$ or $2s^2$ shell of the oxygen ion and provides the creation of two or three electron-hole pairs, respectively. Long-term investigations of α-Al_2O_3 crystals did not lead to the detection of immobile self-trapped holes or electrons. The *A* emission excited at the direct photocreation of excitons or at the recombination of free electrons and free holes is interpreted by us as the radiative decay of self-shrunk excitons. The theoretical model of Sumi allows the existence of such immobile self-shrunk excitons even if an electron and a hole do not separately undergo the self-trapping. [S0163-1829(99)01825-1]

I. INTRODUCTION

Nonrelaxed intrinsic electronic excitations (EE's), which manifest themselves in the reflection spectrum and the spectra of optical constants, have been investigated in detail for single crystals of the wide-gap material α-Al_2O_3 (energy gap $E_g = 9.4$ eV).[1–4] Theoretical calculations of the structure of conduction (CB) and valence bands (VB) in Al_2O_3 have also been done.[5–7] An α-Al_2O_3 single crystal is optically anisotropic and its unit cell contains ten ions. A doublet structure was observed in the region of 8.8–9.3 eV, i.e., at the edge of fundamental absorption of Al_2O_3. A long-wavelength component of this doublet is well pronounced for the electric field of incident light parallel to the optic axis ($\mathbf{E} \| c$), whereas the short-wavelength component dominates in the absorption for incident light with $\mathbf{E} \perp c$.[4] The absorption bands at 8.8–9.3 eV are convincingly interpreted as the formation of p^5s excitons. The hole component of these excitons is formed from *p*-type oxygen VB, while *s*-type CB is responsible for the electron component.[1–4]

A long-term investigation of cubic-alkali-halide crystals (AHC's) with a simpler lattice structure led to the conclusion that intrinsic EE's undergo significant changes between initial photon absorption and the process of EE radiative annihilation. Free excitons (FE's) created by exciting radiation undergo transformation into self-trapped excitons (STE's) in singlet or triplet states (see, e.g., Refs. 8–10, and references therein). An optically formed free hole can be transformed into a self-trapped hole (STH) due to the formation of a dihalide quasimolecule located at two anion sites (V_K center). The recombination of electrons and V_K centers causes the appearance of the recombination luminescence of STE's. A photon with the energy exceeding, by several times, the value of E_g creates in AHC's an electron-hole (e-h) pair with a hot electron whose energy is sufficient for the formation of a secondary e-h pair or a secondary exciton.[11] An analogous process of multiplication of EE's has been revealed in $YAlO_3$ crystals as well.[12]

The studies of the process of relaxation, self-trapping, and multiplication of EE's, formed by 8.5–40-eV photons, have so far been inadequate in anisotropic α-Al_2O_3 crystals. Some technical difficulties are the fact that the main intrinsic emission of sapphire has the maximum at 7.6 eV, i.e., the methods of vacuum-ultraviolet (VUV) spectroscopy were needed for the detection of this luminescence under crystal excitation by x rays[13] or by an electron beam.[14,15] The process of photoexcitation of 7.6-eV emission has been studied even more poorly. It has been shown only that the 7.6-eV emission in Al_2O_3 can be excited by 8.8–9.2-eV photons.[15,16] Photons of such energy cause the creation of excitons.[1–4]

It was supposed that the 7.6-eV emission in α-Al_2O_3 corresponds to the radiative decay of STE's.[13–16] This hypothesis is widely cited in literature. On the other hand, the emission of FE's has not yet been detected in Al_2O_3. The existence of STH's, stable up to 220 K, was assumed in Ref. 16. However, there is no convincing confirmation of the existence of STH's in Al_2O_3. Furthermore, it was shown by the electron-spin-resonance method that the holes, thermal annealing of which occurs at 220 K, are localized near Mg^{2+} impurity ions in Al_2O_3:Mg.[17]

An emission with the maximum in the region of 3.8 eV was observed in Al_2O_3 crystals and tentatively ascribed to

the recombination of electrons and STH's.[16,18] Unfortunately, the α-Al_2O_3 single crystals grown at high temperatures do not have ideal stoichiometric composition. An Al_2O_3 crystal, growing even in a weak reduction regime, provides the formation of anion vacancies, the charge of which is partially compensated by electrons (F^+ and F centers are formed[19]). The luminescence of F^+ centers lies in the region of 3.8 eV also.[20] So, it is difficult to separate the emission of F^+ centers and the supposed luminescence of STE's at 3.8 eV.

Up to now the investigation of low-temperature processes of EE relaxation as well as of the supposed STE emissions was carried out mainly for Al_2O_3 crystals under excitation by x rays, an electron beam, or by VUV radiation of $h\nu < 11$ eV.[13–20] In the present study we investigated the excitation processes of intrinsic and impurity emissions as well as the process of multiplication of EE's in Al_2O_3:Sc crystals and in α-Al_2O_3 crystals of high purity and perfection under excitation by synchrotron radiation (SR) at 8 K. In the region of high absorption constants it is necessary to take into account the complicated processes in near-surface crystal layers of about 1μm thickness (see, e.g., Ref. 3). Therefore, the processes of various luminescence excitation by electron pulses of nanosecond duration have also been studied. The penetration depth of 300-keV electrons in Al_2O_3 is 300 μm.

The main goals of the present study were (i) the experimental investigation of the spectral-kinetic peculiarities of the excitation of the 7.6-eV intrinsic emission and of the 5.6-eV emission of Sc^{3+} centers and (ii) the consideration of the mechanisms of the creation and of the radiative decay of excitons localized in the defectless lattice region.

II. EXPERIMENT

The photoluminescence experiments were carried out at the SUPERLUMI station of HASYLAB at DESY, Hamburg. The experimental setup has been described in Ref. 21. The excitation spectra were normalized to equal quantum intensities of SR falling onto the crystal. A typical spectral resolution of 0.33 nm (about 20 meV in the region of 8.5 eV) was used. The full width at half maximum of SR pulses was 130 ps with the maximum repetition rate of 5 MHz. The excitation spectra were measured for time-integrated luminescence, as well as for the emission detected within a time window (length Δt) correlated with the excitation pulses of SR (delayed by δt). Up to four time windows were set simultaneously. The delay δt and the length Δt were varied between 0.6–60 and 1.5–110 ns, respectively.

The experiments with irradiation by an electron beam were carried out at the Institute of Physics, University of Tartu. The spectra of steady luminescence were measured in the region 1.8–9.0 eV using excitation by 6-keV electrons at 8–300 K. The cathodoluminescence of Al_2O_3 (3.8–9 eV) was recorded through a double vacuum monochromator by a solar-blind photomultiplier in the photon counting regime.[22] A typical optical slit width of monochromator was 13 Å. The spectra of fast emission were measured using a powerful electron pulse generator GIN-600.[23] The duration of a single electron pulse was $\tau = 3$ ns, the current density 1–150 A cm^{-2}, and its average electron energy 300 keV. Fast luminescence was recorded through a monochromator by a system consisting of a photomultiplier EMI 9863 B/Q, a fast oscilloscope, and a telecamera.[24]

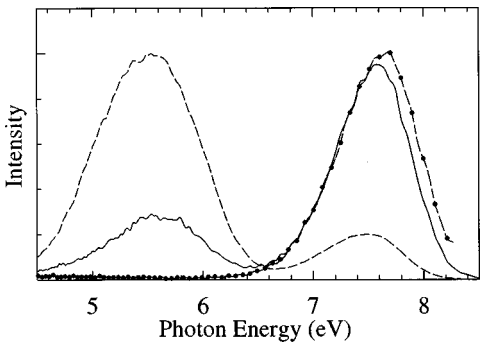

FIG. 1. Luminescence spectra of Al_2O_3 (●), Al_2O_3:Sc (150 ppm, solid line) and Al_2O_3:Sc (600 ppm, dashed line) in the case of excitation by 6-keV electrons at 8 K.

Single Al_2O_3 and Al_2O_3:Sc crystals were the main objects of the present study. The α-Al_2O_3 crystals of high purity and perfection were grown by the Czochralski technique.[25] In the region of extrinsic absorption (2–8.5 eV) the values of the absorption constant do not exceed $k = 1-2$ cm^{-1} at 295 K for our α-Al_2O_3 samples.[26] The Al_2O_3:Sc crystals contained about 150 or 600 ppm of Sc^{3+} ions that substituted aluminum ions. At 8 K, Sc^{3+} impurity ions are responsible for a broad absorption band with the maximum at 8.5 eV adjoining the region of intrinsic absorption. The emission of Sc^{3+} centers (the maximum at $E^I = 5.6$ eV) does not undergo thermal quenching up to 300 K.[27]

The main experiments with SR were carried out for the parallel-sided crystal plates of dimensions $10\times10\times2$ mm^3 with the c axis normal to the excited surface. The excitation spectra were measured at the incidence angle of 17.5°. In some cases the excited surface of Al_2O_3 was parallel to the c axis. In all the cases of electron excitation, an electron beam was oriented at an angle 45° to a crystal surface and the luminescence was detected perpendicular to excitation direction.

III. EXPERIMENTAL RESULTS

A. Luminescence spectra

Figure 1 presents the steady luminescence spectrum of a highly pure Al_2O_3 crystal at 8 K in case of excitation by 6-keV electrons. Analogous emission spectra were obtained if the energy of electrons equaled 9 or 3 keV. A broad luminescence band with the maximum at $E^I = 7.6$ eV (half-width $\delta \approx 0.8$ eV) dominates in the emission spectrum of a pure Al_2O_3 crystal at 8 K. Doping of Al_2O_3 by Sc^{3+} impurity ions (150 ppm) leads to the appearance of a broad emission band $E^I = 5.6$ eV (see Fig. 1). At a higher concentration of Sc^{3+} impurity ions (about 600 ppm) the 5.6-eV emission dominates in the spectrum, while the intrinsic VUV emission is weakened.

Figure 2 shows the luminescence spectra of α-Al_2O_3, Al_2O_3:Sc (150 ppm), and Al_2O_3:Sc (600 ppm) crystals at 8 K in the case of excitation by photons of several energies $h\nu_e$. The luminescence band $E^I = 7.6$ eV dominates in the spectrum of time-integrated photoluminescence at an excitation in the region of the long-wavelength component of the

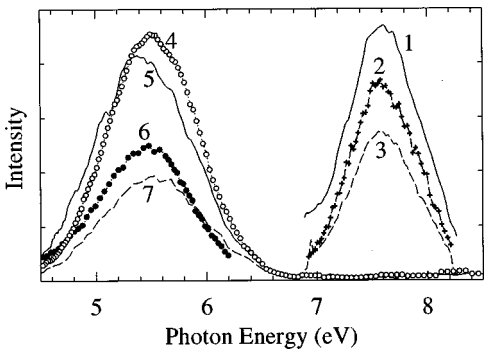

FIG. 2. Luminescence spectra of Al_2O_3 (curves 1–3), Al_2O_3:Sc (150 ppm, curves 4 and 5), and Al_2O_3:Sc (600 ppm, curves 6 and 7) in case of excitation by photons of 8.97 eV (1–3), 8.8 eV (4 and 5), and 10.7 eV (6 and 7) at 8 K (1–4, 6) or 295 K (5 and 7). The spectra are measured for time-integrated (1, 4–7) and fast emissions ($\Delta t = 2.1$ ns, $\delta t = 0.6$ ns, curve 2 and $\Delta t = 23$ ns, $\delta t = 2.6$ ns, curve 3).

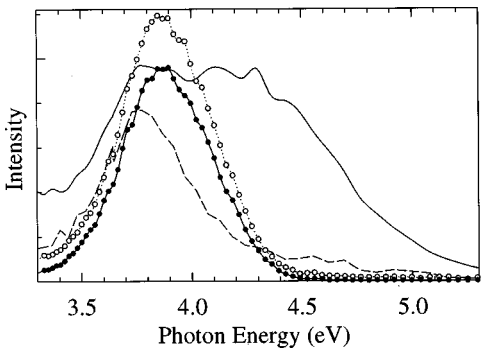

FIG. 3. Luminescence spectra of Al_2O_3 crystals in the case of excitation by 8.97 eV (solid and dashed lines) and 10-eV photons (○ and ●) at 8 K. The spectra are measured for time-integrated (solid curve and ○) and fast emission, $\Delta t = 5$ ns, $\delta t = 1.5$ ns (dashed line and ●).

exciton doublet ($h\nu_e = 8.98$ eV). The spectra of fast luminescence ($\Delta t = 2.1$ ns, $\delta t = 0.6$ ns and $\Delta t = 23$ ns, $\delta t = 2.6$ ns) are practically the same. A large half-width of the so-called *A* luminescence of Al_2O_3 (7.6 eV) testifies to the connection of this emission with the decay of the localized EE's formed after the achievement of the equilibrium distribution of luminescence centers in vibrational energy. Direct excitation of Sc^{3+} centers by 8.5-eV photons causes the appearance of intense luminescence $E^I = 5.6$ eV in Al_2O_3:Sc (150 or 600 ppm). However, in case of 10.7-eV photon excitation *A* emission dominates in Al_2O_3 and Sc^{3+} center emission in Al_2O_3:Sc (600 ppm). The *e*-*h* mechanism of 5.6-eV luminescence excitation is efficient at 295 K. The Al_2O_3:Sc crystal with a sufficiently high-impurity concentration is an effective short-wavelength emitter in a wide temperature region. The third ionization potential of a free scandium atom (24.75 eV) is significantly lower than for an aluminum atom (28.44 eV). Thus, the Sc^{3+} ions that substitute Al^{3+} cations do not serve as electron traps. The analysis of experimental data allows us to conclude that the luminescence of Sc^{3+} centers arises also in the region of band-to-band transitions due to the electron recombination with the holes localized at oxygen ions near Sc^{3+}. The Al_2O_3:Sc excitation by 8.5-eV photons causes the creation of near-impurity EE's that decay later with the appearance of broadband 5.6-eV emission.

The emission band $E^I = 3.8$ eV was also observed in Al_2O_3 at 8 K. The detailed comparison of photoluminescence peculiarities in the region of 3.8 eV for α-Al_2O_3, where the luminescence of F^+ centers was undoubtedly detected,[20] and the so-called *E* emission of STE's is supposed to exist[16,18] was of special interest for us. Figure 3 depicts the luminescence spectra for one of the nominally pure Al_2O_3 crystals in the case of the sample excitation at 8 K by 8.97-eV photons, which selectively generate excitons. The spectrum for the time-integrated emission in the region of 3.3–5.2 eV consists of a number of subbands. However, the emission with the maximum $E^I = 3.77$ eV ($\delta \approx 0.48$ eV) dominates in the spectrum of ''fast'' emission ($\Delta t = 5$ ns, $\delta t = 1.5$ ns). Earlier, a similar emission band ($E^I = 3.8$ eV, $\delta \approx 0.4$ eV at 80 K) was tentatively ascribed to STE luminescence (*E* emission) in α-Al_2O_3.[16,28] On the other hand, this hypothesis was constantly criticized because of the existence of well-established 3.8-eV emission of F^+ centers in Al_2O_3 samples with preirradiation *F* centers. This F^+ center emission could also be excited out of the region of fundamental absorption (selective absorption/excitation bands exist in the transparency region of Al_2O_3 from 4.5 to 8.5 eV).[20]

We succeeded in detecting the fast component of 3.8-eV emission ($\Delta t = 5$ ns, $\delta t = 1.5$ ns), which does not have selective excitation bands from 4.5–8.8 eV and can be excited only at the photocreation of excitons (8.9–9.2 eV) or *e*-*h* pairs ($h\nu > 9.5$ eV). The absence of excitation bands in the region of extrinsic absorption is an important indication of intrinsic luminescence. So, in addition to the intrinsic *A* emission, the 3.77-eV emission is also connected with the radiative decay of excitons in α-Al_2O_3. Further we will use the *E* definition for the second intrinsic luminescence band. Figure 3 demonstrates that the 10-eV photon excitation generating *e*-*h* pairs in Al_2O_3 causes the appearance of the emission band $E^I = 3.87$ eV $\delta \approx 0.5$ eV for both time-integrated and fast ($\Delta t = 5$ ns) signals. The maximum of this recombination luminescence is shifted by 0.1 eV toward higher energies with respect to the fast *E* emission excited at the direct formation of excitons.

B. Spectra of luminescence excitation

Figure 4 shows the excitation spectra of the three main broadband emissions ($E^I = 7.6$, 3.8, and 5.6 eV) measured for Al_2O_3 and Al_2O_3:Sc (160 ppm) crystals at 8 K. In order to facilitate the separation of the spectral region of intrinsic and extrinsic EE's, the solid line reproduces the absorption tail measured for the electric field of incident light $\mathbf{E} \| c$ in Al_2O_3 at 10 K.[4] The absorption tail for $\mathbf{E} \perp c$ is shifted slightly toward the high-energy region (by 70 meV at the value of $k = 10^2$ cm^{-1}).[4] The efficiency of the fast 7.6-eV emission (curves 2 and 3) of high-purity Al_2O_3 is high in the excitation region of 8.9–9.1 eV, where the value of intrinsic absorption varies from 10^1 to 10^4 cm^{-1}. For another Al_2O_3 sample, where the *c* axis was not strictly normal to the excited surface, the region of high efficiency of fast 7.6-eV emission is wider and reaches 9.3 eV ($k = 10^5$ cm^{-1}).

There are no excitation bands in the region of 4.5–8.9 eV (i.e., out of the region of fundamental absorption) in the ex-

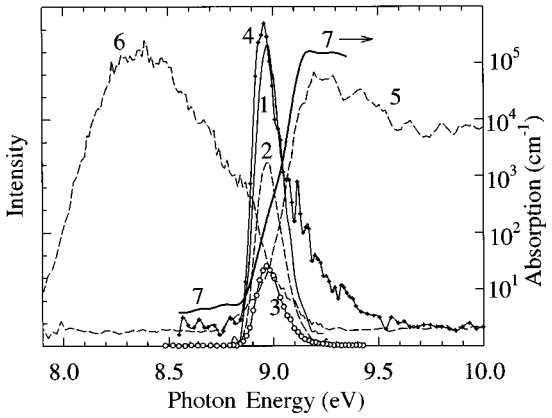

FIG. 4. Time-resolved excitation spectra for Al_2O_3:Sc (150 ppm) and two samples of Al_2O_3 at 8 K. Al_2O_3 No. 1, time-integrated (curve 1) and fast 7.6-eV emission [$\Delta t = 23$ ns, $\delta t = 2.6$ ns (curve 2) and $\Delta t = 2.1$ ns, $\delta t = 0.6$ ns (curve 3)] of STE's. Al_2O_3 No. 2, fast emissions of 7.6 eV [$\Delta t = 23$ ns, $\delta t = 6$ ns (curve 4)] and 3.8 eV [$\Delta t = 5$ ns, $\delta t = 1.5$ ns (curve 5)]. Al_2O_3:Sc, time-integrated 5.6-eV emission of Sc^{3+} centers (curve 6). A fragment of the absorption spectrum (curve 7) of Al_2O_3 ($\mathbf{E} \| c$) (Ref. 4).

citation spectrum of fast 3.8-eV emission ($\Delta t = 5$ ns, $\delta t = 1.5$ ns) for an Al_2O_3 crystal of high purity and perfection. The efficiency of fast 3.8-eV emission $\eta_{3.8}$ reaches the maximum value at 9.2 eV and is still high in the region of interband transitions ($h\nu > 9.5$ eV). So, the maximum of 3.8-eV emission efficiency lies at higher exciting photon energy (by 0.2 eV) than that of 7.6-eV luminescence. It is necessary to mention that the F^+ center 3.8-eV band in an F^+-rich crystal reaches its excitation maximum at 4.8 eV, i.e., at the direct photoexcitation of F^+ centers, but is several times weaker in the region of fundamental absorption. This sample of Al_2O_3 was grown in a reduced regime and contains a large number of F^+ and F centers.

According to Fig. 4, the emission of Sc^{3+} centers ($E^I = 5.6$ eV) can be effectively excited by 8.0–8.8-eV photons, while the value of η_{Sc} is low in the region of 9.1–10 eV. The 5.6 eV emission can also be excited in the region of a long-wavelength component of exciton absorption (8.9–9.1 eV), partly due to the reabsorption of A luminescence by Sc^{3+} centers.

The analysis of the excitation spectra for the fast components of 3.8- and 7.6-eV emissions, and their comparison with the previously measured spectra of intrinsic optical constants,[2,4] allows us to conclude that the A band at 7.6 eV and a part of the E band at 3.8 eV are caused by the radiative decay of optically generated excitons. Photoexcitation in the region of a long-wavelength component of the exciton absorption leads mainly to the appearance of 7.6-eV emission, while 3.8-eV luminescence dominates in the short-wavelength component of an exciton absorption (9.1–9.4 eV). Because of the relatively weak excitation provided by our experimental conditions, the 7.6-eV emission practically cannot be excited by photons of $h\nu > 9.5$ eV at the experimental station used. However, the excitation of Al_2O_3 by an intensive line of krypton discharge (10 eV) leads to the appearance of the 7.6-eV luminescence.[18]

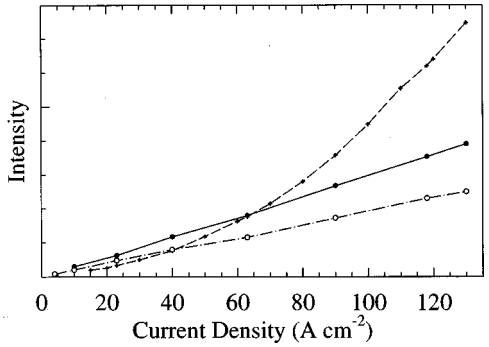

FIG. 5. Dependencies of emission intensity on the current density of nanosecond 300-keV electron pulses at 80 K: 7.6-eV emission of STE's in Al_2O_3 (×), 4.15-eV emission of STE's in KI (●), and 5.6-eV emission of Sc^{3+} centers in Al_2O_3:Sc (○).

C. The dependence of the emission intensity on the excitation density

The dependencies of the intensity of several intrinsic and impurity emissions on the density of excitation by nanosecond electron pulses have been studied for nominally pure Al_2O_3 crystals of various origins as well as for Al_2O_3:Sc crystals. Figure 5 presents some of these dependencies measured for Al_2O_3 and Al_2O_3:Sc (600 ppm) at 80 K by means of single electron pulses (300 keV, $\tau = 3$ ns) with the change of current density from 1 to 150 A cm^{-2}. The intensity of Sc^{3+} center emission depends linearly on the density of excitation while the intensity of STE A emission increases approximately quadratically with the increasing electron current density. This behavior is observed in a wide temperature range although the A emission of STE's at 295 K is thermally quenched by two orders of magnitude with respect to the luminescence intensity at 80 K. The superlinear dependence was detected for steady 7.6-eV emission under a 6-keV electron-beam excitation at 8 K.

Generally, the dependence of the intensity of recombination luminescence I_L on the excitation intensity (density) I_e consists of three main stages. At low values of I_e, when the separate excited regions of a crystal do not overlap, there is a linear dependence between I_L and I_e (the so-called first linear region). At the second stage of $I_L = f(I_e)$ the overlapping of the excited regions in a crystal takes place causing an increase of the average excitation density. In the case of the existence of the rival recombination channels to the luminescence investigated, the dependence between I_L and I_e is usually quadratic. At even higher values of I_e, when the number of e-h pairs formed at the excitation significantly exceeds the number of rival recombination centers, the dependence of $I_L = f(I_e)$ is linear again (the second linear region). So, the two linear stages of $I_L = f(I_e)$ are separated by the region of the superlinear dependence of the luminescence intensity on the excitation density. The dependence of $I_L = f(I_e)$ has been thoroughly investigated (both experimentally and theoretically) for several phosphors on the base of wide-gap crystals, used in selective dosimeters (see, e.g., Ref. 29). In relatively pure sapphire crystals with the content of impurity recombination centers about 10 ppm, the excitation of A emission due to the recombination of e-h pairs formed by SR in our experimental conditions occurs within the first linear region. The excitation of Al_2O_3 by powerful nanosecond electron

pulses with the current density 3–90 A cm^{-2} corresponds to the superlinear dependence between I_L and I_e (see Fig. 5). At higher current density (10^2-10^3 A cm^{-2}) the second linear region of $I_L=f(I_e)$ can also be realized.

To compare the behavior of STE emission in Al_2O_3 and AHC's we measured the dependence of STE σ emission (4.15 eV) intensity on the current density of single electron pulses for a KI crystal (the content of impurity ions was 3–10 ppm) at 80 K. This dependence appears to be linear (see Fig. 5). It was proved unambiguously that the σ emission of STE's in KI is caused by the recombination of electrons with STH's (V_K centers) stable at 80 K. The linear dependence for Sc^{3+} center emission in Al_2O_3:Sc (600 ppm) is connected with the migration of electrons and holes at 10–15 interion distances that provides the efficient excitation of 5.6-eV emission of Sc^{3+} centers in a crystal with high-impurity concentration. If holes underwent fast self-trapping and STE emission arose due to the recombination of electrons with STH's, the linear dependence on the excitation density would be valid also for the intensity of STE emission in an Al_2O_3 crystal. However, our experiments revealed no linear dependence for the *A* emission of STE's. Furthermore, *A* emission was not detected in any peak of thermally stimulated luminescence connected with the release of electrons from impurity traps and their recombination with holes. We performed special experiments with Al_2O_3, Al_2O_3:Sc, and Al_2O_3:Ga crystals and did not observe the 7.6-eV thermally stimulated luminescence at the heating of the electron-irradiated crystal from 8 to 295 K. There are no manifestations of the freezing of STE *A* emission intensity at a cooling of an Al_2O_3 crystal, irradiated by 9-eV photons, down from 80 to 4 K. So, contrary to the case of exciton self-trapping in alkali iodides,[8] the transformation of a free exciton into a self-trapped state in Al_2O_3 is not impeded by an activation barrier.

D. Multiplication of EE's in Al_2O_3 and Al_2O_3:Sc

The effect of the multiplication of free *e*-*h* pairs in narrow-gap semiconductors was investigated in detail (see, e.g., Ref. 30). Another mechanism of the multiplication of EE's (MEE) has been detected in wide-gap dielectrics. A photon with the energy exceeding the threshold value creates an *e*-*h* pair in which the energy of a hot conduction electron is sufficient to form a secondary exciton.[11]

In the case of Al_2O_3, the excitation of cerium center emission was investigated long ago in an Al_2O_3:Ce cathodoluminophor at 295 K. There were no manifestations of the MEE process in the region of exciting photon energy up to 21.2 eV.[31] Figure 6 shows the excitation spectrum of Sc^{3+} center emission (time-integrated luminescence of 5.6 eV was detected through a monochromator) measured in the region of 7–37 eV for Al_2O_3:Sc (600 ppm) at 8 K. The emission of Sc^{3+} centers can be efficiently excited within the region of Sc^{3+} center absorption (7–8.8 eV) as well as at the formation of intrinsic EE's of Al_2O_3 by 8.8–37-eV photons. The absorption spectrum of α-Al_2O_3 at 295 K ($\mathbf{E}\perp c$) (Ref. 4) is reproduced in Fig. 6 as well. Photons of 9.5–11 eV provide the electron transitions from a valence band into a lower *s*-type subband of CB. In this case, the value of η_{Sc} is approximately only a half of that at the direct excitation of

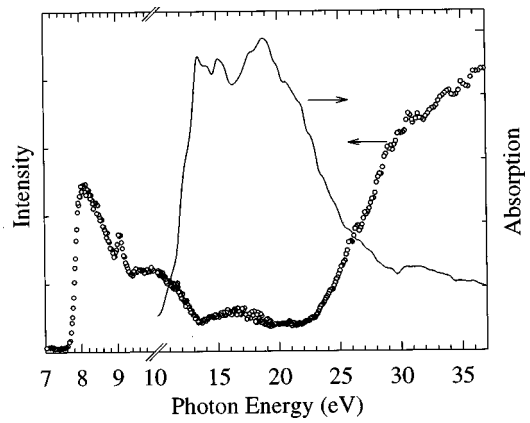

FIG. 6. Excitation spectra of 5.6-eV emission of Sc^{3+} centers for Al_2O_3:Sc (600 ppm) at 8 K. A fragment of the absorption spectrum of an Al_2O_3 crystal ($\mathbf{E}\perp c$) (Ref. 4).

Sc^{3+} by 8.0–8.9-eV photons totally absorbed by the crystal. In the region of 12–24 eV the value of reflectivity *R* varies from 20% to 35% and the depth of penetration of the exciting photons into a crystal is small ($r=10^{-5}-10^{-6}$ cm). Therefore, the value of η_{Sc} is lower in this spectral region. The influence of near-surface nonradiative recombination and reflection losses significantly decreases starting from 25 eV ($R<10\%$, $r\approx10^{-3}$ cm) down to the level typical of the 9.5–11-eV region. The value of η_{Sc} sharply increases from 25 to 37 eV exceeding even the efficiency of Sc^{3+} center emission at the direct photoexcitation of Sc^{3+}. In order to explain this increase of η_{Sc}, it is necessary to take into account that the values of *k* for 11- and 29-eV photons are practically equal,[4] while the value of η_{Sc} at least doubles from 11 to 29 eV. The value of *k* is practically constant in the region of 29–37 eV; however, a sharp increase of the efficiency of Sc^{3+} center emission continues in this spectral region as well. Therefore, the increase of η_{Sc} at 26–37 eV cannot be explained by a trivial reduction of near-surface losses. The analysis of the data presented in Fig. 6 allows us to conclude that the absorption of one photon of 26–29 eV leads to the creation of two *e*-*h* pairs, while one photon of 30–37 eV creates up to three *e*-*h* pairs. The following recombination of these *e*-*h* pairs at Sc^{3+} centers causes the appearance of the 5.6-eV impurity luminescence with $\eta_{Sc}>1$. This is the so-called effect of photon multiplication in an optical spectral region observed earlier in a number of AHC's.[32]

The reflection of incident light and near-surface nonradiative losses were taken into account at the interpretation of the excitation spectra for impurity emissions in a MgO:Al crystal.[33] The used corrections smoothed the value of η in a wide region of fundamental absorption (8–20 eV), while the value of η increases, nevertheless, three times at $h\nu>20$ eV. The process of MEE in Al_2O_3 takes place at $h\nu>25$ eV. The higher threshold energy for MEE in Al_2O_3 is caused by higher value of the energy gap (9.4 and 7.8 eV in Al_2O_3 and MgO, respectively).

Figure 7 shows the excitation spectrum for the time-integrated and fast ($\Delta t=5$ ns, $\delta t=1.5$ ns) emissions of 3.8 eV measured in Al_2O_3 at 8 K. The fast emission can be excited in the region of fundamental absorption ($h\nu>8.8$ eV) only. On the other hand, the time-integrated signal

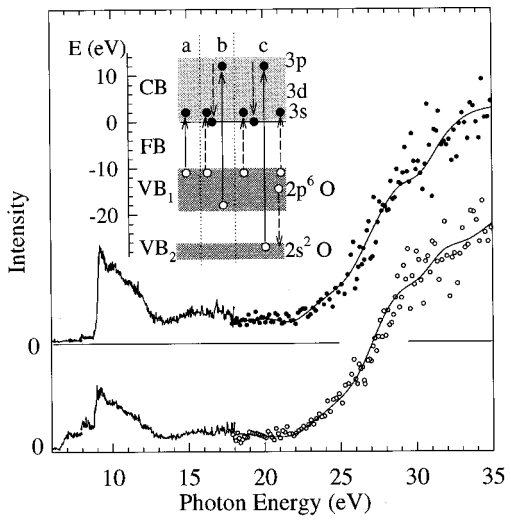

FIG. 7. Excitation spectra for the time-integrated (○) and fast ($\Delta t = 5$ ns, $\delta t = 1.5$ ns) emission (●) of 3.8 eV in a Al_2O_3 crystal at 8 K. Inset shows a simplified energy-band diagram of an Al_2O_3 crystal (see text for details).

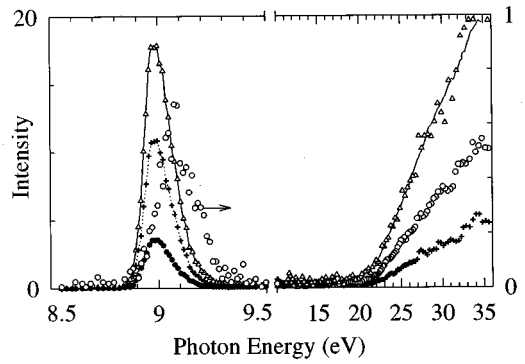

FIG. 8. Excitation spectra for the time-integrated (△), fast [$\Delta t = 13.8$ ns, $\delta t = 2.4$ ns (●) and $\Delta t = 43$ ns, $\delta t = 15.5$ ns (+)] and slow ($\Delta t = 110$ ns, $\delta t = 56$ ns) components (○) of *A* emission in an Al_2O_3 crystal at 8 K. The right intensity scale is valid for the 10–37-eV region, and the left scale for the low-energy region (except for the curve marked by an arrow). All the lines are guide lines.

at 3.8 eV consists of several spectrally close components and its excitation spectrum has weak bands at $h\nu < 8.8$ eV. Similar to an Al_2O_3:Sc crystal (see Fig. 6), the sharp increase of 3.8-eV emission efficiency at 25–37 eV is the manifestation of the MEE process in Al_2O_3, while low values of η_E at 12–24 eV are caused by the effective near-surface losses due to the nonradiative recombination of electrons and holes in this spectral region. The coincidence of the excitation spectra for fast and steady emissions of 3.8 eV in the region of MEE is an additional proof of the Auger-type mechanism of the MEE process.

The inset in Fig. 7 shows a simplified energy-band diagram of an Al_2O_3 crystal based on theoretical calculations.[5–7] VB_1 and VB_2 are two valence subbands formed by $2p^6$ and $2s^2$ states of oxygen ions, respectively. The experimentally determined values of $E_g = 9.4$ eV (Ref. 18) and band width for VB_1 (7–9 eV) and VB_2 (3–4 eV) (Ref. 34) are used in our schematic diagram. The complicated CB is formed by $3s$, $3d$, and $3p$ states of aluminum ions (the lowest part of CB is connected with $3s$ states).[6] According to Ref. 6, the lower part of VB_1 is a mixture of $2p^6$ and $2s^2$ states of oxygen because of the partial covalency of Al_2O_3. It causes the high probability of electron transitions from the lower part of VB_1 to the $3p$ region of CB. Just such transitions are responsible for the formation of secondary *e-h* pairs: the energy of a hot conduction electron, formed after photon absorption, is sufficient to create the second *e-h* pair while a hot hole in VB_1 is not able to form a secondary EE (case *b* in the diagram). The value of threshold energy for this MEE process, $E_t = 25$ eV, significantly exceeds $2E_g \approx 18.8$ eV because a significant part of the absorbed energy of an exciting photon is transferred to a photohole. The case *c* in the diagram illustrates the situation when the energy of the absorbed photon equals 35–36 eV. The ionization process starts from the $2s^2$ shell of an oxygen ion and stops in the $3p$ region of CB. A hot photoelectron in CB is able to form the second *e-h* pair, while the Auger recombination of an electron from $2p^6$(O) with a $2s$(O) hole provides the creation of the third *e-h* pair. So, the absorption of one 35–36-eV photon leads to the creation of three *e-h* pairs. Our interpretation of the MEE process in Al_2O_3 is qualitative, and further precise calculations of the band structure are needed.

IV. ABOUT MECHANISMS OF EXCITON SELF-TRAPPING IN Al_2O_3

The creation mechanisms of the excitons localized in a regular lattice are of special interest. According to Fig. 4 the efficiency of the *A* emission is especially high at the excitation in the long-wavelength region (8.85–9.1 eV) of the exciton absorption. At least three components, the duration of which is ~20, ~200, and ~2000 ns, can be distinguished within the *A* emission excited by x-ray pulses.[35] Nevertheless, the nature of these components is still unclear. We investigated the decay kinetics of the 7.6-eV emission in Al_2O_3 after excitation by 8.97-eV photons that cause the direct optical formation of excitons. The intensity of the *A* emission decreases by two orders of magnitude during the first 50 ns although a weak slow component remains up to 200 ns (the limit of our time-resolved measurements).

Figure 8 presents the excitation spectra of the *A* emission (7.5-eV emission was detected through a monochromator) measured in the spectral region of 8.5–36 eV at 8 K. The spectra were measured for steady (time-integrated) luminescence as well as for the emission components detected within several time windows. Two fast components ($\Delta t = 13.8$ ns, $\delta t = 2.4$ ns and $\Delta t = 43$ ns, $\delta t = 15.5$ ns) are excited in the region of 8.85–9.15 eV and their efficiency maximum is situated at 8.97 eV. The efficiency maximum for a slow component ($\Delta t = 110$ ns, $\delta t = 56$ ns) is shifted toward the higher energy. The analysis of the data presented in Fig. 8 allows us to conclude that the excitation spectra of the *A* emission have a fine structure: a fast emission dominates in the long-wavelength region of the exciton absorption, while a slow emission dominates in the short-wavelength region.

In alkali iodides, the lowest-energy state of p^5s excitons corresponds to pure triplet paraexcitons and singlet excitons are mainly created in the short-wavelength region of the exciton absorption.[9,10] The spin-orbit splitting for p^5s excitons

in MgO is by an order of magnitude smaller than in iodides and the lowest-energy state is ascribed to a singlet state.[36] In Al_2O_3, a nanosecond component of the 7.6-eV emission is efficiently excited in the long-wavelength region of exciton absorption. A component with nanosecond duration is usually typical of singlet exciton emission. So, our experimental results testify that the lowest state of p^5s excitons in α-Al_2O_3 is a singlet state mainly.

The efficiency of time-integrated and fast ($<$50 ns) components of the *A* emission in the region of 35 eV is 20 times as low as that at the direct optical creation of excitons by 8.97-eV photons (see Fig. 8). One photon of 35 eV is able to form three *e*-*h* pairs (see Sec. III D). So only 2% of *e*-*h* pairs formed by 35-eV photons recombine with the appearance of the fast components of *A* emission. However, the efficiency of slow *A* emission ($\Delta t = 110$ ns, $\delta t = 56$ ns) of triplet excitons at 35 eV reaches the same value as in the region of direct optical formation of excitons by 9.1–9.15 eV.

The process of exciton self-trapping in α-Al_2O_3 significantly differs from that in a number of AHC's where it was investigated in detail.[8,9] In AHC, the emission of STE can be excited at the direct optical creation of excitons as well as in the region of interband transitions at the recombination of electrons with relaxed immobile V_K centers.[8–10] According to Fig. 5 the intensity of STE emission in KI depends linearly on the density of excitation by 300-keV electrons. An effective cross section for the electron recombination with immobile V_K centers is large ($\sigma = 3\times10^{-12}$ cm^2). The efficiency of 4.15-eV STE emission in KI at the direct photocreation of excitons or at the recombination of electrons with immobile V_K centers is practically the same.

The behavior of *A* emission in Al_2O_3 drastically differs from that of STE emission in KI. The efficiency of *A* emission at the excitation by 9.5–10.5-eV photons in the region of band-to-band transitions (where $k < 10^5$ cm^{-1} and the probability of near-surface nonradiative recombination is low) is about 100 times as low as at the direct creation of excitons by 8.98-eV photons (see Fig. 4 and 8). The recombination creation of *A* emission is efficient only under the excitation by powerful electron pulses (see Fig. 5). The difference between the behavior of *A* emission in Al_2O_3 and 4.15-eV STE emission in KI we ascribe to the fundamental difference of hole processes in these two crystals.

In contrast to AHC's and SiO_2 the long-term search for immobile self-trapped holes in Al_2O_3 was unsuccessful (see, e.g., Ref. 37). In the close-packed oxygen sublattice of Al_2O_3 holes migrate even at 4 K so rapidly that they are able to cause neither a large displacement of neighboring ions, nor even a strong polarization of a lattice. Moreover, even in crystals with the total content of imperfections of about 10 ppm, the holes undergo localization mainly near various impurity ions or defects. The role of electron recombination with holes that undergo intermediate localization at impurities (defects) becomes negligible if a single electron pulse forms more than 10^{18} *e*-*h* pairs in 1 cm^3 of an excited crystal. In such conditions of excitation, the recombination of electrons and holes efficiently causes the formation of excitons in regular lattice. Our estimation shows that the needed excitation density can be provided if the current density of electron pulses exceeds 80 A cm^{-2}, i.e., when ''the second linear region'' of excitation is reached (see Sec. III C).

The half-width of the long-wavelength component of the exciton absorption band in Al_2O_3 is about 0.15 eV at 8 K, which is not typical of large-radius Wannier excitons. On the other hand, the integral exciton absorption is smaller than it is expected to be for small-radius Frenkel excitons. The binding energy of p^5s excitons in Al_2O_3 is $E_B \approx 0.3$ eV. So, the excitons, the effective average radius of which exceeds the interanion distance (2.5–2.8 Å) approximately 5 times, are probably formed in an Al_2O_3 crystal. The translational mass of such excitons is significantly larger than the effective mass of a hole. The migration of excitons through a crystal lattice is relatively slow; therefore they undergo a localization in the defectless regions of a crystal and after vibrational relaxation decay with the appearance of *A* emission. The quantum yield of *A* emission at the excitation by 9-eV photons at 5 K was estimated as $\eta_A \geqslant 0.25$.[15,18] Heating of a crystal up to the temperature of $T > 80$ K causes a significant increase of the absorption in the region of the Urbach tail of an exciton band. This increase is connected with the enhancement of the exciton interaction with phonons the effective energy of which is $\hbar\omega_{\rm eff} \approx 31-34$ meV.[4,15] According to our data, the dependence of the half-width of *A* emission on the temperature in the region of 80–300 K can also be described as an interaction with phonons of $\hbar\omega_{\rm eff} \approx 38$ meV. In Al_2O_3, the value of $\hbar\omega_{\rm eff}$ at the creation of excitons and at their radiative decay corresponds to the acoustic branch of vibrations. The vibration spectrum of Al_2O_3 was investigated by means of neutron scattering at 20 K.[38]

Our experimental data testify to the excitation of the *A* emission not only at the direct formation of p^5s excitons by 8.9–9.3-eV photons but also at the recombination of free electrons and free (mobile) holes. However, the effective cross section σ for the recombination of free electrons and holes in a regular lattice of Al_2O_3 is significantly lower than that value for the *e*-*h* recombination near neutral Sc^{3+} centers ($\sigma \approx 10^{-15}$ cm^{-2}). In KI, the value of $\sigma \approx 10^{-12}$ cm^{-2} is typical of the recombination of electrons and immobile self-trapped holes. The efficiency of the recombination mechanism of the excitation of *A* emission is high only at a sufficiently high density of *e*-*h* pairs formed at the excitation.

Experimental results can be interpreted within the bounds of the Sumi diagram for the possible interaction of intrinsic EE's with the field of acoustic phonons.[39] This phase diagram was later applied for the description of the behavior of EE's in regular lattice of various solids (see, e.g., Refs. 10, 18, and 40). In the case of large- and medium-radius excitons, phonons effect both the center-of-mass (translational) motion and the relative (internal) motion of electron and hole components of an exciton. Sumi considered four possible phases for an electron and a hole interacting in the acoustic-phonon field.[39] The realization of the definite phase in solids of various classes depends on the electron-phonon and hole-phonon interaction, the ratio of the effective masses for carriers, and the sign of deformation potentials of an electron and a hole. In semiconductors, there exist free electrons, holes, and excitons, while none of them was detected in a self-trapped state. In AHC's, electrons do not undergo the self-trapping, but holes and excitons exist in both free and self-trapped states. Self-trapped electrons as well as self-

trapped holes have been recently detected in lead halides.[41]

According to Sumi, one more unusual situation is possible: an electron and a hole do not separately undergo transformation into a stable self-trapped state while the sum of their deformation potentials is sufficient for the recombination formation of a localized exciton. The formation of such excitons is accompanied by the shrinking of wave functions of an electron and a hole that take place in recombination. Therefore, such unusual localized excitons were named as self-shrunk excitons (SSE's). SSE's were supposed to exist in Y_2O_3 (Ref. 40) and Al_2O_3.[18] Our experimental results, presented in this paper, confirm the interpretation of the intrinsic *A* emission in Al_2O_3 as the radiative decay of SSE's. In contrast to STE emission in AHC's, the *A* emission was not detected in any peak of thermally stimulated luminescence recorded at the heating of irradiated Al_2O_3 crystals (of various levels of purity and perfection) from 8 to 350 K. So, the recombination component of *A* emission is not connected with the so-called ''recombination through a local center'' and should be considered as the result of the recombination of free electrons and mobile holes. Similar to many semiconductors, the probability of *e*-*h* recombination is low (at least in the regime of relatively weak excitation).[42]

It is necessary to mention that neither self-trapped holes nor self-trapped electrons have been yet detected in cubic face-centered MgO crystals. On the other hand, the intense edge emission of free excitons (7.69 eV) has been revealed in MgO, although (in contrast to Al_2O_3) there is no broadband emission connected with STE's in this system.[43] In uniaxial BeO crystals, the emission of FE's is very weak, while the two intense emission bands (with the maxima at 4.9 and 6.7 eV) that correspond to the two configurations of excitons, localized in regular lattice, have been detected.[44] The reduced symmetry of α-Al_2O_3 and BeO wide-gap oxides promotes the formation of stable STE's. Unfortunately, the theory of SSE's in low-symmetry crystals has not yet been elaborated.

ACKNOWLEDGMENTS

This work was supported by the Estonian Science Foundation (Grant No. 3868) and the PECO Program. M.K. is grateful for financial support from the STINT Foundation (Sweden).

[1] E. T. Arakawa and M. W. Williams, J. Phys. Chem. Solids **29**, 735 (1968).

[2] V. N. Abramov, M. G. Karin, A. I. Kuznetsov, and K. K. Sidorin, Fiz. Tverd. Tela (Leningrad) **21**, 80 (1979) [Sov. Phys. Solid State **21**, 47 (1979)].

[3] M. L. Bortz, R. H. French, D. J. Jones, R. V. Kasowski, and F. S. Ohuchi, Phys. Scr. **41**, 537 (1990).

[4] T. Tomiki, Y. Ganaha, T. Shikenbaru, T. Futemma, M. Yuri, Y. Aiura, S. Sato, H. Fukutani, H. Kato, T. Miyahara, A. Yonesu, and J. Tamashiro, J. Phys. Soc. Jpn. **62**, 573 (1993); T. Tomiki, Y. Ganaha, T. Futemma, T. Shikenbaru, Y. Aiura, M. Yuri, S. Sato, H. Fukutani, H. Kato, T. Miyahara, J. Tamashiro, and A. Yonesu, *ibid.* **62**, 1372 (1993).

[5] S. Ciraci and I. P. Barta, Phys. Rev. B **28**, 982 (1983).

[6] W. Y. Ching and Y.-N. Xu, J. Am. Ceram. Soc. **77**, 404 (1994).

[7] Y.-N. Xu, Z.-Q. Gu, X.-F. Zhong, and W. Y. Ching, Phys. Rev. B **56**, 7277 (1997).

[8] Ch. B. Lushchik, in *Excitons*, edited by E. I. Rashba and M. D. Sturge (North-Holland, Amsterdam, 1982), Chap. 12.

[9] K. S. Song and R. T. Williams, *Self-Trapped Excitons* (Springer-Verlag, Berlin, 1993).

[10] Ch. B. Lushchik and A. Ch. Lushchik, *Decay of Electronic Excitations with Defect Formation in Solids* (Nauka, Moscow, 1989).

[11] A. Lushchik, E. Feldbach, R. Kink, Ch. Lushchik, M. Kirm, and I. Martinson, Phys. Rev. B **53**, 5379 (1996), and references therein.

[12] Ch. Lushchik, E. Feldbach, A. Frorip, M. Kirm, A. Lushchik, A. Maaroos, and I. Martinson, J. Phys.: Condens. Matter **6**, 11 177 (1994).

[13] W. A. Runciman, Solid State Commun. **6**, 537 (1968).

[14] A. I. Kuznetsov, I. L. Kuusmann, M. I. Musatov, A. A. Ratas, and V. N. Abramov, Pis'ma Zh. Tekh. Fiz. **3**, 60 (1976) [Sov. Tech. Phys. Lett. **3**, 60 (1977)].

[15] A. Kuznetsov, B. Namozov, and V. Mürk, Proc. Acad. Sci. Estonian SSR, Phys. Math. **36**, 193 (1987).

[16] P. Kulis, Z. Rachko, M. Springis, I. Tale, and J. Jansons, Radiat. Eff. Defects Solids **119/121**, 963 (1991).

[17] H. A. Wang, C. H. Lee, F. Kröger, and R. T. Cox, Phys. Rev. B **27**, 3821 (1983).

[18] A. I. Kuznetsov, V. N. Abramov, V. V. Mürk, and B. P. Namozov, Fiz. Tverd. Tela (Leningrad) **33**, 2000 (1991) [Sov. Phys. Solid State **33**, 1126 (1991)].

[19] I. I. Milman, V. S. Kortov, and S. V. Nikiforof, Radiat. Meas. **29**, 410 (1998).

[20] B. D. Evans and M. Stapelbroek, Phys. Rev. B **18**, 7089 (1978).

[21] G. Zimmerer, Nucl. Instrum. Methods Phys. Res. A **308**, 178 (1991).

[22] I. Kuusmann, P. Liblik, R. Mugur, V. Tiit, E. Feldbach, R. Shatskina, and J. Edula, Trudy Inst. Fiz. Akad. Nauk Estonian SSR **51**, 57 (1981).

[23] B. N. Kovalchuk, G. A. Mesyats, B. N. Semin, and V. G. Shpak, Prib. Tekh. Eksp. **4**, 15 (1981).

[24] K. U. Ibragimov and F. A. Savikhin, Fiz. Tverd. Tela (Leningrad) **35**, 1474 (1993) [Sov. Phys. Solid State **35**, 744 (1993)].

[25] M. I. Musatov and L. I. Belevtseva, Izv. Akad. Nauk SSR, Neorg. Mater. **12**, 358 (1976) [Inorg. Mater. **12**, 311 (1976)].

[26] V. N. Abramov, B. G. Ivanov, A. I. Kuznetsov, I. A. Meriloo, and M. I. Musatov, Phys. Status Solidi A **48**, 287 (1978).

[27] A. I. Kuznetsov, V. N. Abramov, V. V. Mürk, B. R. Namozov, and T. V. Uibo, in *Proceedings of the International Conference on Lasers, 1981*, edited by C. B. Collins (STS Press, McLean, VA, 1981), pp. 793–796.

[28] J. L. Jansons, P. A. Kulis, Z. A. Rachko, M. J. Springis, I. A. Tale, and J. A. Valbis, Phys. Status Solidi B **120**, 511 (1983).

[29] G. S. Zavt and F. A. Savikhin, Izv. Akad. Nauk SSSR, Ser. Fiz. **38**, 1325 (1974).

[30] W. Shockley, Czech. J. Phys., Sect. B **11**, 81 (1961); V. S. Vavilov, J. Phys. Chem. Solids **8**, 223 (1959); A. N. Belski, V.

V. Mikhailin, and A. N. Vasil'ev, Radiat. Eff. Defects Solids **135**, 383 (1995).
[31] E. R. Ilmas and T. A. Savikhina, J. Lumin. **1/2**, 702 (1970).
[32] E. R. Ilmas, G. G. Liidya, and Ch. B. Lushchik, Opt. Spektrosk. **18**, 453 (1965) [Opt. Spectrosc. **18**, 255 (1965)].
[33] A. N. Vasil'ev, V. N. Kolobanov, I. L. Kuusmann, Ch. B. Lushchik, and V. M. Mikhailin, Fiz. Tverd. Tela (Leningrad) **27**, 2696 (1985) [Sov. Phys. Solid State **27**, 1616 (1985)].
[34] S. P. Kowalczyk, F. R. McFeely, L. Ley, V. T. Gritsyna, and D. A. Shirley, Solid State Commun. **23**, 161 (1977).
[35] V. V. Myurk and K. M. Ismailov, Fiz. Tverd. Tela (St. Petersburg) **35**, 498 (1993) [Phys. Solid State **35**, 259 (1993)].
[36] R. C. Whitel, C. J. Flaten, and W. C. Walker, Solid State Commun. **13**, 1903 (1973).
[37] R. C. Hughes, Phys. Rev. B **19**, 5318 (1979); P. Martin, S. Guizard, Ph. Daguzan, G. Petite, P. Auderbert, J. P. Greindre, A. Dos Santos, and A. Antonetti, Europhys. Lett. **29**, 401 (1995).
[38] H. Bialas and H. J. Stolz, Z. Phys. B **24**, 319 (1975).
[39] A. Sumi, J. Phys. Soc. Jpn. **43**, 1286 (1977).
[40] Ch. B. Lushchik, Izv. Akad. Nauk Latvian SSR, Ser. Fiz. Tekh. Nauk **N2**, 57 (1984).
[41] S. V. Nistor, E. Goovaerts, M. Stefan, and D. Schoemaker, Nucl. Instrum. Methods Phys. Res. B **141**, 538 (1998).
[42] R. H. Bube, *Photoelectronic Properties of Semiconductors* (Cambridge University Press, Cambridge, 1992).
[43] E. H. Feldbach, Ch. B. Lushchik, and I. L. Kuusmann, Pis'ma Zh. Eksp. Teor. Fiz. **39**, 54 (1984) [JETP Lett. **39**, 61 (1984)].
[44] V. Yu. Ivanov, V. A. Pustovarov, S. V. Gorbunov, S. V. Kudyakov, and A. V. Kruzhalov, Fiz. Tverd. Tela (St. Petersburg) **38**, 3333 (1996) [Phys. Solid State **38**, 1818 (1996)].